Science of Sintering, **51** (2019) 409-419

doi:https://doi.org/10.2298/SOS1904409P

UDK: 553.532; 532.528; 622.785

The Mechanisms of Cavitation Erosion of Raw and Sintered Basalt

Marko Pavlović[1], Marina Dojčinović[1], Radica Prokić-Cvetković[2], Ljubiša Andrić[3*)]

[1]University of Belgrade, Faculty of Technology and Metallurgy, Karnegijeva 4, 11000 Belgrade, Serbia

[2]University of Belgrade, Faculty of Mechanical Engineering, Kraljice Marije Street 16, 11000 Belgrade, Serbia

[3]Institute for Technology of Nuclear and Other Mineral Raw Materials, Franchetd'Esperey 86, 11000 Belgrade, Serbia

Abstract:

The paper analyzes the morphology of cavitation damage of raw and sintered basalt samples. The experiment was conducted using the ultrasonic vibratory cavitation test method according to the ASTM G-32 standard. During the determination of the resistance to the effect of cavitation, a change in the mass of samples was observed in the function of the cavitation time of operation. The morphology of damage caused by the effect of cavitation was followed by scanning with an electron microscope, and the level of degradation of the surface of the samples was quantified using the image analysis. The results showed a significantly higher degree of resistance of sintered basalt, with a cavitation rate of 0.019 mg/min relative to raw basalt, with a cavitation rate of 0.738 mg/min. After 120 minutes of exposure to the cavitation effect, a smaller number of small pits on the surface of sintered basalt were observed, while a higher level of damage to the surface with the appearance of numerous pits was found in raw basalt, which can be connected in some places to larger and deeper pits in some places. The obtained results indicate the possibility of using sintered basalt for the production of parts that will be exposed to the effects of high cavitation loads.

Keywords*: Raw basalt; Sintered basalt; Cavitation damages; Mass loss; Image analysis.*

1. Introduction

Basalt is a hard, compact, basic volcanic rock. It usually contains plagioclases, pyroxene and olivine, and often has a glassy appearance [1-4]. It is a cheap and widespread raw material for the production of glass and glass ceramics by the processes of sinter crystallization, melting, casting and thermal treatment. Glass-ceramics based on basalt have a very fine and homogeneous structure, excellent physical and mechanical properties, chemical resistance, high wear and corrosion resistance and can replace metallic materials in the construction of structural parts of equipment in metallurgy and mining [5-11]. Technical ceramic based on basalt find application in all industrial branches where the problem with the chemical resistivity and wearability is actual: electrical engineering, chemical engineering, metallurgy and mining [12-18]. According to the literature, in the world, basalt is used as a raw material for the production of basalt wool, thin and super thin basalt fiber, cast products,

*) **Corresponding author:** lj.andric@itnms.ac.rs

basalt plastics, anti-corrosive materials, building materials, thermal insulation materials [19-22]. For general application, basalt is used for making porcelain, majolica, faience, sanitary ceramics, art ceramics, for making decorative furniture, dishes, glazes for decoration of various ceramic and other products [23, 24]. Synthesis and application of composite materials with a polymeric base and a basalt based reinforcing (basalt fibers, basalt powder) are widely present in the mechanical engineering, automative, shipbuilding, construction industry for the construction of parts and equipment where high hardness and wear resistance are required [25-28]. Thanks to its superior features glass-ceramics based on basalt can be used in environments in which erosion wear, corrosion, high temperatures and pressures are present, the action of aggressive chemicals and suspensions, fluid flow [29-31]. Laboratory tests of the cavitation resistance of the raw and sintered basalt were made to evaluate the possibility of basalt application from the Vrelo Kopaonik deposit for the production of industrial equipment parts and applications in similar exploitation conditions. An ultrasonic vibration method with a stationary sample was used for testing [32]. The purpose of the laboratory method of cavitation damage testing is to predict the behavior of the material during the cavitation operation for a shorter test period (2 - 10 h), and the advantages of the method are small size of the device, small sample size for testing, low energy input. During the cavitation, the process of formation, growth and implosion (collapse) of steam or vapor gas bubbles in the flowing fluid takes place. During bubble collapse, high temperatures and pressures are generated locally (approximately 5000 ^{o}C and 1000 bar) in a very short period of time (less then 1μs). Implosion of bubbles creates shock waves and micro-yets, which cause mass loss and damage to the surface of materials with which the liquid is in contact [29, 33-35]. To estimation the cavitation resistance of basalt samples, a change in the mass of samples was observed in the function of the exposure time to the effect of cavitation. Also, the level of sample surface degradation was monitored using an image analysis program, Image Pro Plus [36]. On the basis of the obtained results, a comparison of the properties of the tested samples was performed and an assessment of the possibility of their application for the given exploatation conditions.

2. Materials and Experimental Procedures

2.1. Synthesis and Characterization

Basalt rocks from the Vrelo Kopaonik deposit were used as the starting material for the preparation of samples for testing. Raw basalt samples (sample mark: RB) dimensions (15x15x15) mm are cut from the selected basalt rocks. The basic characteristics of basalt which influenced his choice for exploring cavitation resistance and assessment of application in engineering practice were: melting point 1300-1400 ºC; high hardness 6.5-7 Mosh scale; density 2460-2960 kg/cm^3; basically amounts of glass 10-15 %; high tensile strength; compressive strength 80 MPa; porosity 3,78%; high resistance to acids, alcalines and heat; high thermal conductiviy; no cancerogenic risk or other health hazards; completly inert with no environmental risk [1-4].

By crushing and milling the basalt rocks, a basalt aggregate of grain size below 1 mm was obtained. Table I shows the chemical composition of the starting basalt sample. The basalt aggregate is ground in a vibrating mill with spherical balls at a grain size of 15μm. The obtained basalt powder is mixed with pressing additives (0,6 % bentonite; 0,5 % cellulose). The test specimens were pressed into plates of dimensions (100x50x15) mm using Leitz pressure device with applied presure of 10^6 Pa. Afterwards, the basalt samples were sintered at temperature of 1150 ºC. The sintering regime process was carried out according to the following mode: raising the temperature to 1000 ºC with a heating rate of 5 ºC/min in a time of 200 min; then, heating up to 1150 ºC with heating rate of 2 ºC/min in a time of 100 min; sintering at 1150 ºC in a time of 1 hour. Sample mark of sintered basalt: SB.

Tab. I Chemical composition of the raw basalt sample (%).

Sample	SiO_2	Al_2O_3	Fe_2O_3	FeO	MgO	CaO	Na_2O	K_2O	TiO_2
Raw basalt	56.21	18.61	1.15	2.97	3.40	7,78	4.73	3.37	1.11

Basalt samples were analyzed using X-ray diffractometer, ″Philips″ model PW-1710. The microstucture of the samples was characterized with the scanning electronic microscope JEOL model JSM 6610 LV. In order to improve conductivity, the sample was vapoured with gold powder.

2.2 Methods

2.2.1 Cavitation erosion testing

An ultrasonic vibratory cavitation test method (with a stationary sample) was used to test cavitation resistance according to the standard ASTM G-32 [32] and the procedure described in earlier works [29, 33]. Testing was performed within the recommended standard values of the following parameters [32, 34]:

- the frequency of mechanical vibrations: 20±0,2 kHz;
- the amplitude of vibrations at the top of the transformer: 50 μm;
- gap between the test specimen and the transformer: 0,5mm;
- water flow rate of 5-10 ml/s;
- the water temperature in the bath: 25±1 ^{o}C.

Selected time of sample testing was (min): 15; 30; 60; 120. After each test interval, a change in the mass of the samples was measured by analytical balance with an accuracy of ±0,1mg. For the purpose of analyzing the surface changes under cavitation, the samples were photographed before, during and at the end of the test.

2.2.2 Image analysis

Software sample analysis was performed in Image Pro Plus [36]. The results of the analysis enabled the examination of the mechanisms of formation and development of damage to the surface of the tested samples under the effect of cavitation. The following indicators of surface damage were observed: the level of degradation of the sample surface, (P/P_0, %, where P_0 refers to the reference surface without damage, and the value P represents damage on the surface of the sample formed during the test), the number of formed individual pits, N_p and medium area of formed pits, P_{av} (mm^2). The formation of new pits, their growth and / or their interconnection was monitored. The resulting damage on the surface of the samples was analyzed based on the corresponding line profiles obtained using the Image Pro Plus image analysis software program. All obtained results of damage to the surface of the samples at the time of the cavitation activity are illustrated by the diagrams.

The morphology of the damaged surfaces of the speciment was analyzed by a scanning electron microscopy (SEM) Joel JSM 6610 LV.

3. Results and Discussion

3.1. Phase composition of basalts samples

The mineral composition of raw basalt (RB) and sintered basalt (SB) are as follows: plagioclases, pyroxenes, olivines, Figure 1. The most prevalent minerals in the RB sample are basic plagioclases, while pyroxene (augit) and olivine are less present, Figure 1a. Figure 1b

shows feldspats and pyroxene in the analyzed sample SB. Feldspats (basic plagioclases) are significantly more prominent than pyroxene (diopside).

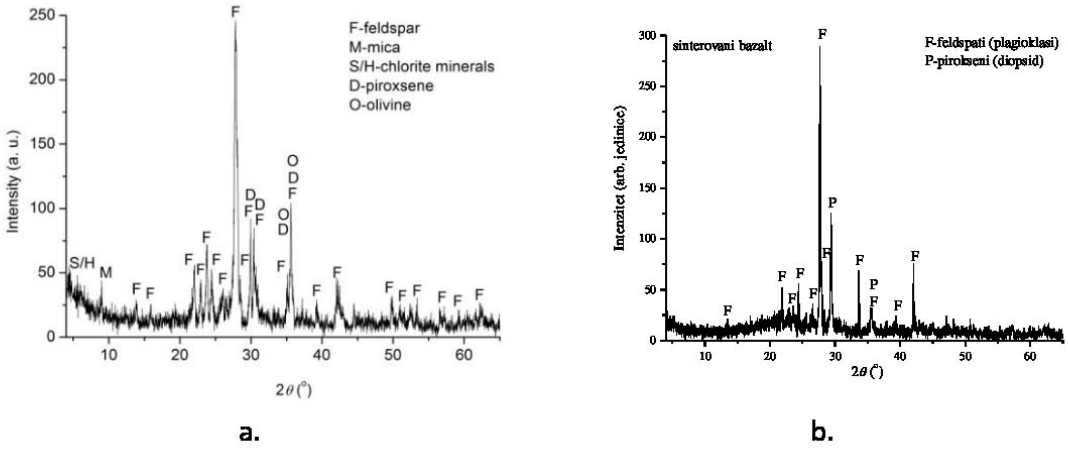

Fig. 1. XRD of basalt samples: a. raw basalt; b. sintered basalt.

3.2. Microstructural analysis of basalt samples

In Figure 2, SEM microphotographs of the RB and SB samples are shown before the cavitation process. The base of the examined sample of raw basalt, Figure 2a, was constructed from a microcrystalline plagioclase with a microlitic structure. From fenocrystals, olivines, rhombic pyroxene and rarely basic plagioclases have been identified. The basalt rock structure is represented by olivine-pyroxene basalt. In the structure of sintered basalt, evenly distributed crystals of plagioclase and pyroxene are present in the basic mass of the sample, Figure 2b. The structure of RB and SB samples contains bubbles of various sizes, wich are filled with air or glass, Figure 3. The present bubbles on the surface of the samples cause surface roughness and the appearence of pits. RB sample contains a large number of tiny bubbles, Figure 3a, while the SB samples contained bubbles of larger dimensions that are embedded in the cryptocrystalline-glass base, Figure 3b.

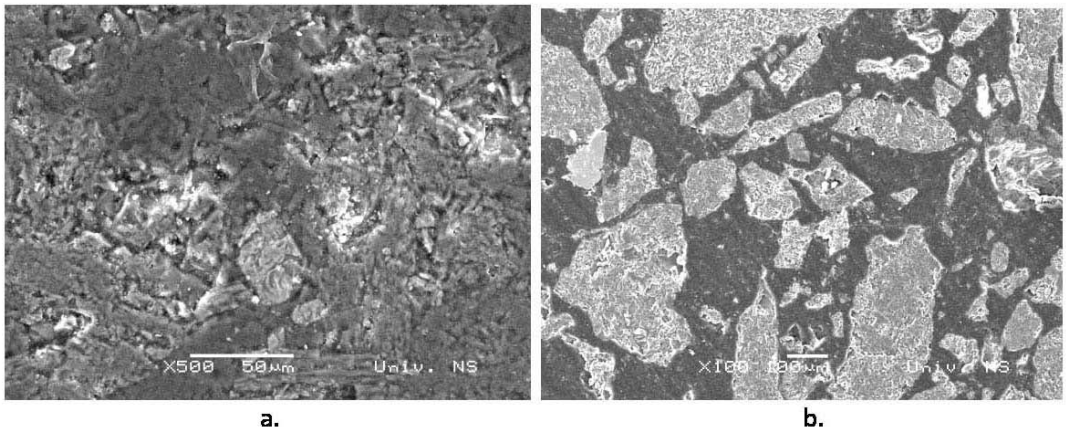

Fig.2. SEM microphotographs of basalt samples: a. raw basalt; b. sintered basalt.

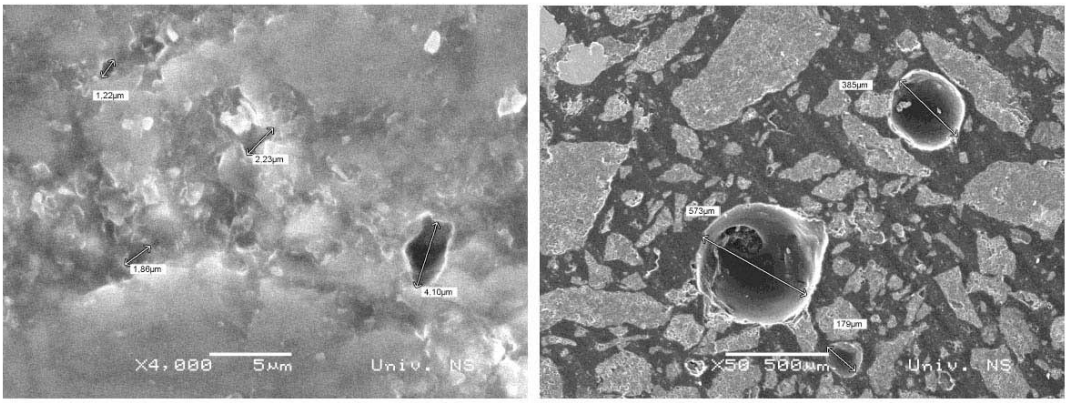

Fig.3. The present bubbles in the basalt structure: a. RB sample; b. SB sample.

During the cavitation test, the changes of the present bubbles contained in the basalt base, as well as the present pits on the surface of the sample RB and SB were monitored.

3.3. Mass change

Measurement of the mass loss of samples under the effect of cavitation during the test time is shown in Figure 4. The mass loss resulting from cavitation damage is applied to the ordinate, and the time intervals are displayed on apcis. It has been shown that the SB samples have a significantly higher cavitation resistance with a cavitation rate of 0.019 mg/min compared to RB samples with a cavitation rate of 0.738 mg/min. Analyzing the progression of erosion of SB samples, it can be concluded that the mass loss is small, in the first 15 min the mass loss is 0,91 mg and slightly increases to mass loss of 2,26 mg for 120 min of exposure. In RB samples, it is evident that the incubation period at the early stage of the damage is short, because the period without mass loss is almost negligible. According to the selected test conditions in the first 15 min, the mass loss of the RB sample is up to 15 mg, and as the exposure time increases, the cumulative mass loss of the sample gradually increases, almost linearly to 88.5 mg in 120 min of exposure.

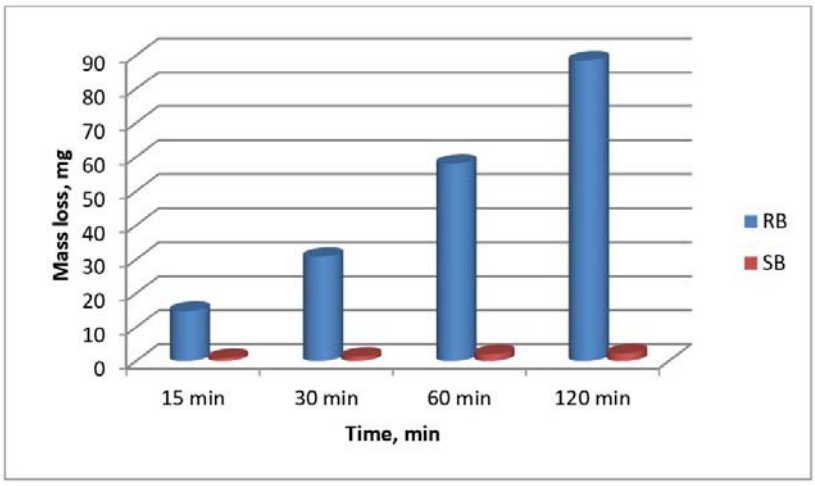

Fig. 4. Mass loss of basalt samples during the cavitation erosion testing: RB-raw basalt; SB-sintered basalt.

A higher level of surface damage of RB samples can be interpreted by the rough structure of the raw basalt sample in relation to the fine-grained and homogeneous structure of the SB samples.

3.4. Image analysis

Figure 5 shows photographs of RB and SB samples during a cavitation test with corresponding profile lines obtained using image analysis using Image Pro Plus [36]. It was noted that the SB sample exhibits less surface damage than the RB samples and there is almost no change in the dimensions of the pits that existed on the surface of the sample prior to testing. The profile lines of SB sample are uniform, and individual peaks, which are present at the same locations on the surface of the sample refered presence of individual pits, caused by the presence of bubbles in the structure, which were identified prior to the start of the test. On the RB sample the initial pits on the surface and the present roughness are changing and increasing the dimensions during cavitation exposure time, which can be seen in the major changes on the profile lines of RB sample during testing.

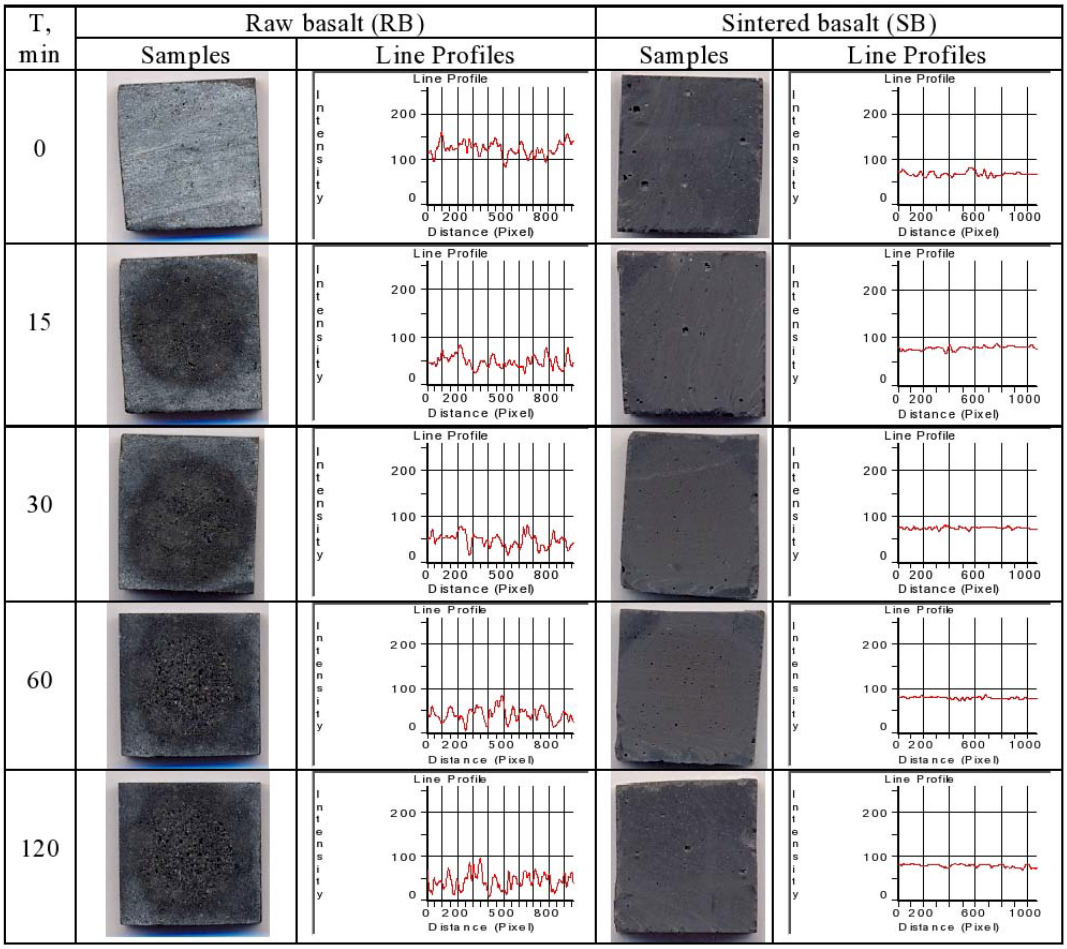

Fig. 5. Photographs of raw and sintered basalt samples before and during the cavitation erosion testing after implementation of red filter and corresponding line profiles.

The results shown in Figure 5 correspond to the results of damage to the surface of RB and SB samples determined by applying image analysis on photographs of sample surfaces during the cavitation time, processed and analyzed using the Image Pro Plus software, shown in Figure 6.

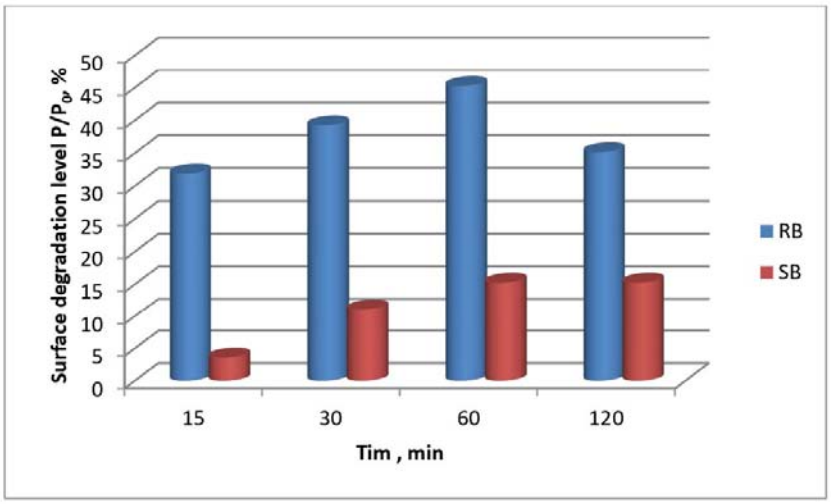

Fig. 6. Surface degradation level of raw and sintered basalt samples during the cavitation erosion testing: RB- raw basalt; SB- sintered basalt.

At the end of 120 min test of SB samples, small changes were observed on the surface of the sample, with a significantly smaller number of small pits in relation to the RB samples in which the surface was damaged in a higher degree with the appearence of a plurality of pits that in some places interconnected in larger and deeper pits. This corresponds with the results of a gradual loss of sample mass during testing, Figure 4. At the end of cavitation exposure damage to the surface of SB sample is 15 %, while damage to RB samples is greater than 35 %, shown in Figure 6. This corresponds the results of determining the average surface of the formed pits, P_{av} shown in Figure 7.

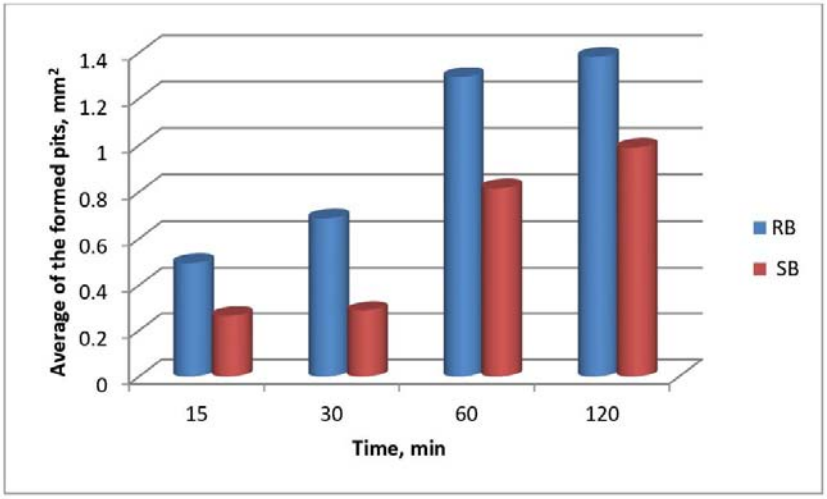

Fig. 7. Average area of the formed pits: RB- raw basalt; SB- sintered basalt.

Figure 8 shows the dynamics of the formation of pits on the surface of RB and SB samples during exposure to cavitation effect.

In the RB sample there are numerous small bubbles in the structure (Figure 3a), which form a multitude of small pits on the surface of the sample, which affects the increase in the roughness of the surface. By the operation of the cavitation process the number of newly formed pits gradually increases. The occurrence of the connection of the pits to the

larger and deeper pits affects the increase in damage on the surface of the sample, Figure 7 (after 120 minutes of cavitation operation the damage of the surface is 35 %, Figure 6). In the SB samples there are individual larger bubbles in the structure (Figure 3b), there are individual larger and smaller pits on the surface of the sample before the beginning of the cavitation operation. During the effect of cavitation, a small number of pits on the sample surface are formed near the already existing bubbles, Figure 8. Formed pits slowly change the surface during the effect of cavitation, Figure 7. The analysis of the SB samples showed that the initial pits on the surface of the sample were most likely due to the presence of bubbles in the structure, do not change during exposure, as can be seen on photographs of SB samples during testing. Creating a smaller number of pits creates less damage to the surface area of the SB samples, so that after 120 minutes of cavitation operation the surface damage is below 15 %, Figure 6.

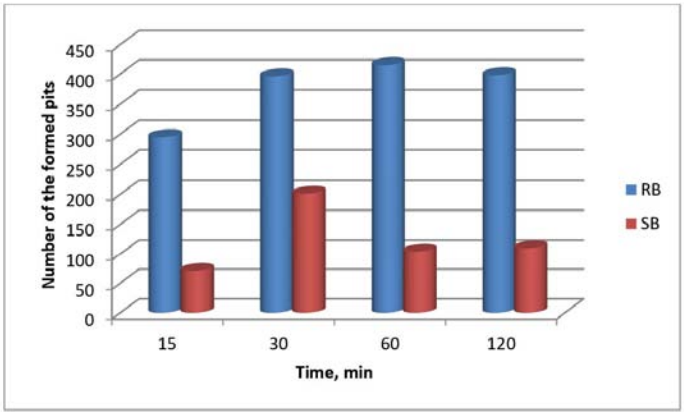

Fig. 8. Number of the formed pits: RB- raw basalt; SB- sintered basalt.

The change in the morphology of the sample surface RB and SB with the test time was followed by scanning electron microscopy, Figures 9 and 10.

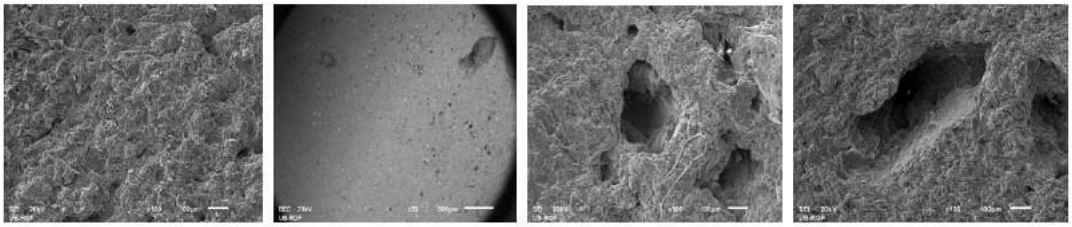

Fig. 9. SEM microphotography of the deformed surfaces of the RB sample with different magnitudes and cavitation effects.

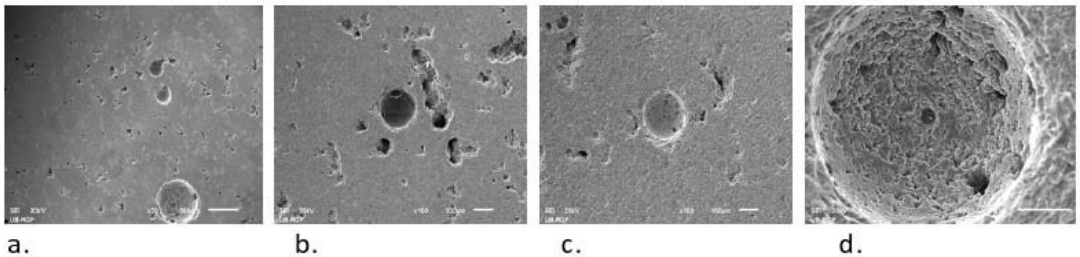

Fig. 10. SEM microphotography of the deformed surfaces of the SB sample with different magnitudes and cavitation effects.

On the surface of the RB sample in the first 15 minutes of the cavitation operation, shallow pits are formed and the roughness of the surface is increasing, Figure 9a. For 30 minutes of cavitation operation, a greater number of pits are formed near the already existing bubble, Figure 9b. During the 60 minute cavitation operation, the appearance of the surface of the existing bubble changes slightly, the pits formed near the bubbles are increased, Figure 9c. The surfaces of already existing bubbles are slightly changed during cavitation operation for 120 min, Figure 9d.

On the surface of the SB sample in the first 15 minutes of the cavitation effect there was no change in the surface area of the sample, Figure 10a. With the effect of cavitation for 30 minutes, small pits are formed near the existing bubbles, Figure 10b. With the effect of cavitation for 60 minutes, Figure 10c, there is no major change in the formed pits and the existing bubble. Bubble areas are very little changed during the effect of the cavitation, for 120min, Figure 10d.

4. Conclusion

The effects of the ultrasonic vibratory cavitation test method for the determination of cavitation damage of the raw and sintered basalt were studied in this paper. The aim was to determine the possibility of using these samples based on basalt to obtain the wear resistant construction elements of equipment in metallurgy and mining which are exposed to high cavitation loads. Analysis of mass loss and progression of erosion of sample surface during the cavitation process showed different effects of cavitation damage of raw basalt samples and sintered basalt samples:

- The mass loss of raw basalt samples in the first 15min of selected test conditions is up to 15 mg, and as the exposure time increases, the cumulative mass loss of the sample gradually increases, almost linearly to 88.5 mg in 120 min of exposure, with a cavitation rate of 0,738 mg/min and total surface area damage of 35 %.
- Analyzing the progression of erosion samples of sintered basalt, it can be concluded that the mass loss is small, in the first 15 min the mass loss is 0,91mg and slightly increases to a mass loss of 2,26 mg for 120 min of exposure, with a cavitation rate of 0.019 mg/min and total surface damage of the sample surface less than 15 %.
- The raw basalt samples compared to sintered basalt samples have got the higher erosion rate, and that can be interpreted by the rough structure of the olivine-pyrroxene basalt from Vrelo-Kopaonik deposit, compared to the compact structure of the obtained sintered samples, with homogenous structure, very great hardness.
- The change in the morphology of the surface of the samples followed by scanning electron microscopy. The damage of the surface of the raw basalt samples begins with the appearance of a large number of small pits on the surface of the sample. By further exposure these pits increase and in some places interconnect and form larger and deeper pits that damage the surface of the samples. On sintered basalt samples, tiny pits appear on the surface only after 30 minutes of exposure. The pits change the shape and dimensions very little until the end of the test. In both samples, it was found that, with prolonged cavitation (120 min), there is an increase in the erosion of the surface of the pits formed near the present bubbles in the base of the basalt. The increase in the erosion of surfaces damaged by bubble during cavitation has not been established.
- The results have enabled the evaluation of the quality of the samples studied and form the basis for the development of basaltic product aquisition technologies by the sintering process. Serbia has significant reserves of quality basaltic rocks, but lacking the developed technologies and adequate production capacity for processing basalt raw materials. The technologies for the production of basalt products by casting and sintering are enviromentally clean, and basalt products are not carcinogenic. It has been shown that sintered basalt samples

based on olivine-pyrroxene basalt from the test deposit can be applied in conditions in which high cavitation loads are expected.

Acknowledgments

The present research was financed by the Ministry of Education, Science and Technological Development of the Republic of Serbia as part of projects TR 35002 and 34006 for which the authors are grateful.

5. References

1. C. Parmelee, Ceramic Glases, M. Deker, Chicago, 1986.
2. W. D. Kingery, H. K. Bowen, D. R. Ulhman, Introduction to Ceramics, a Wiley – Interscience Publication, John Wiley & Sons, Inc., New York, 1976.
3. G. H. Beall, H.L. Rittler, Am Ceram Soc Bull, 55 (1976) 579–82, ISBN ISSN 0002-7812.
4. Barth T. F., Theoretical petrology, John Wiley and Sons Inc., New York-London, 1952.
5. B. Matović, S. Bošković, J.Serb.Chem.Soc. 68 (6) (2003) 505-510.
6. M. Cosić, M. Logar, B. Marović, V. Poharc- Logar, Sci. Sinter. 42 (2010) 383-388.
7. Z. Nikolić, K. Shinagawa, Sci. Sinter. 49 (2017) 1-10.
8. Parra Parra, M. Vlasova, P. Antonio Márquez Aguilar, T. Tomila, Sci. Sinter. 49 (2017) 207-224.
9. M. Cocić, M. Logar, S. Erić, V. Tasić, S. Dević, S. Cocić, B. Matović, Sci. Sinter. 49 (2017) 431-443
10. Lj. Kostić–Gvozdenović, R. Ninković, Inorganic Chemical Technology, Faculty of Technology and Metallurgy, Belgrade, 1997.(In Serbian)
11. R. Simic, N.Gilic, in: Conference Rock, Arandelovac, 2000, Proceedings, p. 150-155.
12. A. Prstic, Z.Aćimovic-Pavlovic, M. Cosic, Lj.Andric, Z. Aćimovic, in: XI Balkan Mineral Processing Congress, Tirana, Albania, 2005, p.422-425.
13. R. Simic, A. Prstic, N. Gilic, in: Conference -Cement 2002, Struga-Macedonia, 2002, Proceedings, p.156-160.
14. Z. Aćimović, Lj. Andrić, V. Milošević, S. Milićević, in: IX Simposium Metals and Nonmetals, Zenica, B&H, 2012, Proceedings, p. 150-155.
15. D. Čikara, A. Todić, D. Čikara-Anić, FME Trans., 38 (2010) 203-207.
16. E. Ercenk, S. Ugur, S. Yilmaz, Ceram. Int., 37 (2011) 883-889.
17. S. Yılmaz, G. Bayrak, S. Sen, U. Sen, Mater. Des., 27 (2006) 1092-1096.
18. A. Karamanov, M. Pelino, J Non-Cryst Solids, (1-3) (2001) 281 139-51.
19. M. Pavlović, M. Sarvan, F. Klisura, Z. Aćimović, in: 4th Conference Maintenace 2016, Zenica, BiH, 2016, Proceedings, p. 175-183.
20. S. Marica, in: Bulletin of the Geological Society of Greece 2004, 36, Proceedings of the 10th International Congress, Thessaloniki, Greece, 2004, pp. 104-108.
21. N.I. Kharbediya, V.M. Bakhtadze, Glass and Ceramics, 8 (1967) 43-44.
22. Prstic A, R. Simic, Lj. Andric, Z. Acimovic, in: Mineral Processing in 21stCentury –X Balkan Mineral Processing Congress, Varna, Bulgaria, 2003, Proceedings, p. 893-897.
23. Lj. Andrić, Z. Aćimović-Pavlović, M. Trumić, A. Prstić, Z. Tanasković, Mater. Des., 33 (2012) 9-13.
24. M. Pavlović, M. Đuričić, A. Mumđić, in: SED 2015, Užice-Srbija, 2015, Proceedings, p. 53-60.

25. V. Fiore, G. Di Bella, A. Valenza, Mater. Des., 32 (2011) 2091-2099.
26. MT Dehkordi, H. Nosraty, MM. Shokrieh, G. Minak, D. Ghelli, Mater. Des., 31(2010) 3835-44.
27. A. Todic, B. Nedeljkovic, D. Cikara, I. Ristovic, Mater. Des., 32 (2011) 1677-1683.
28. Karmanov A., S. Ergul, M. Akyiliz, M. Pelino, J Non-Cryst Solids 354 (2008) 290-295.
29. M. Dojčinović, Chem.Ind. 67 (2) (2013) 323-330.
30. M. Dojčinović, S. Marković, J.Serb.Chem.Soc. 71 (8-9) (2006) 997-984.
31. J. P. Franc, J. M. Michel (Eds), Fundamentals of cavitation, Series Fluid Mechanics and Its Applications, Kluwer Academic Publiser, New York (2004), p.306.
32. Standard Method of Vibratory Cavitation Erosion Test, G32-92. Annual Book of ASTM Standards, Vol. 03.02. Philadelphia: ASTM; 1992.
33. M. Dojčinović, PhD Thesis, University of Belgrade, Faculty Technology and Metallurgy, 2007.
34. M. Dojčinović, Mater.Sci.-Poland 26 (2011) 216-222.
35. G. Garcı́a-AtanceFatjó, M. Hadfield, K. Tabeshfar, Ceram. Int. 37 (2011) 1919-1934.
36. Image Pro Plus, The Proven Solution for Image Analysis, Media Cybernetics, 1993.

Садржај: *У раду је анализирана морфологија кавитационог оштећења узорака ровног и синтерованог базалта. Експеимент је вођен применом ултразвучне вибрационе методе према стандарду АСТМ Г-32. Током одређивања отпорности на дејство кавитације праћена је промена масе узорака у функцији времена деловања кавитације. Морфологија оштећења насталог дејством кавитације праћена је скениг електронским микроскопом, а ниво деградације површине узорака квантификован је применом анализе слике. Резултати су показали знатно већи степен отпорности синтерованог базалта, са кавитационом брзином 0,019мг/мин у односу на ровни базалт, са кавитационом брзином 0,738 мг/мин. После 120 минута излагања дејству кавитације уочен је мањи број ситних јамица на површини синтерованог базалта, док је код ровног базалта констатован већи степен оштећења површине са појавом бројних јамица, које се на појединим местима међусобно спајају у веће и дубље јамице. Добијени резултати указују на могућност примене синтерованог базалта за израду делова који ће бити изложени дејству високих кавитационих оптерећења.*

Кључне речи*: ровни базалт, синтеровани базалт, кавитациона оштећења, губитак масе, анализа слике.*